WILL CLUSTER MORPHOLOGY MEASURES WORK AT STAR?

STARNOTE 0357

L.D.Carr, I.Sakrejda, and T.A.Trainor

University of Washington
Nuclear Physics Lab
Box 354290
Seattle, WA 98195

Lawrence Berkeley National Laboratory
Bldg. 50A-1148
Berkeley, California 94720

July 25, 1998

Abstract

The feasability of adapting NA49 cluster morphology measures to STAR TPC hit reconstruction is examined. Such measures provide a wealth of information about cluster shapes. It is found that the cuts resulting from these measures permit the cluster deconvolution algorithm in the hit finder to search 45% less clusters in the inner sector and 15% less clusters in the outer sector without appreciable loss of efficiency. Because this algorithm is computationally expensive, these measures represent a substantial savings in event reconstruction time. Furthermore they have applications in identifying secondaries and improving χ^2 fits for tracks, in estimating dip and crossing angle, and in event by event physics.

1 Introduction

For algorithmic reasons the track reconstruction in the STAR TPC is done in two stages. The first stage finds where the particles have passed through two dimensional pad vs. time slices and is called hit reconstruction. This two dimensional reconstruction may be subdivided into two further stages. In the first stage contiguous regions of charge in pad-time space are found. These regions are termed clusters. In the second stage, the clusters are deconvoluted into individual hits and each hit is assigned a place in position space. This process is called hit finding.

One cluster may contain information about the passage of several particles.

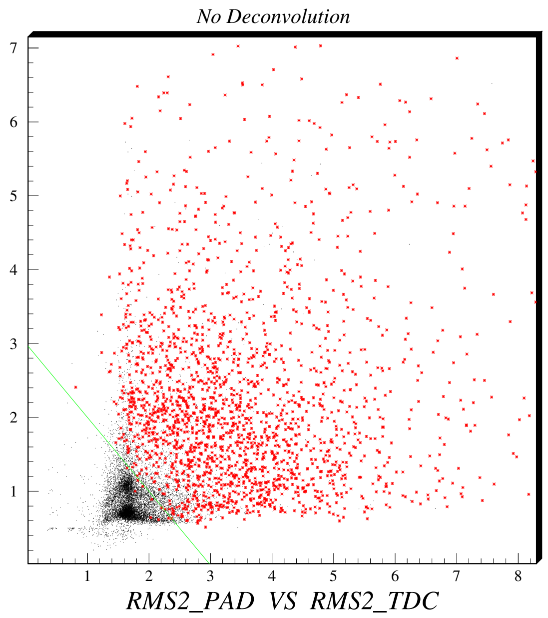

Figure 1: Triage Cut as shown in starnote 0238, courtesy of Mike Lisa

Noise and resolution limits must also be considered. Because of the tremendous data volume which STAR produces, optimization of algorithms is paramount. The cluster and hit finder codes[1] are under evaluation by several people in the TPC group. In the current implementation of the hit finder code, if clusters fail to pass a criterion based on their second moments in pad and time directions, known as the triage cut (Fig. 1), they are characterized as possibly containing more than one hit and are subsequently searched by a computationally expensive peak finding algorithm, known as the mountain finder[2]. The mountain finder in turn is limited by the Raleigh Criterion.

In a previous experiment, NA49, the relativistic heavy ion group at the University of Washington Nuclear Physics Lab found that clusters could be successfully characterized by quadrupole moments and various other morphology measures[3]. In NA49 this greatly increased efficiency of hit finding and decreased processor time[4]. Thus an initial analysis of the feasibility of applying the NA49 morphology measures to the STAR TPC was completed and these measures were then compared to the triage cut currently in use.

The measures were written into an algorithm, called the TPC Cluster Characterization module (TCC), to go between the cluster finder and the hit finder. Because this analysis was only intended to determine if the measures were applicable in STAR, the code was not optimized and the various cuts were made by eye. As it is the collective authors' opinion that TCC should become a standard part of the TPC event reconstruction chain, suggestions are made at the end of the paper for improvements and an optimized version is being written.

2 Mathematical Definitions of the Morphology Measures

The information which comes from the cluster finder code is pad position ($x_{i,j}$), time position ($t_{i,j}$), and pixel charge ($q_{i,j}$), also known as adc value, where both pad and time position are defined on a binned space each element of which is called a pixel. Time has 512 bins over about 2.1 meters for inner and outer sectors. Pad has from 88 to 144 bins, depending on the pad row, from 0.3 to 0.96 meters. For further information see the TPC specs available from STAR home $->$ group documents $->$ TPC $->$ hardware.

First define the normed weights for the pixels contained in each cluster:

$$Q = \sum_{i,j} q_{i,j} \tag{1}$$

$$p_{i,j} = \frac{q_{i,j}}{Q} \tag{2}$$

Find the mean pad and time position:

$$< x >= \sum_{i,j} x_i \, p_{i,j} \tag{3}$$

$$< t >= \sum_{i,j} t_i \, p_{i,j} \tag{4}$$

Find the pad, time, and pad-time variances, which will be used to determine the first quadrupole moment. The detector's pad-time coordinate system is called (x_1, t_1).

$$\sigma^2_{x_1} = \sum_{i,j} (x_i - < x >)^2 \, p_{i,j} \tag{5}$$

$$\sigma^2_{t_1} = \sum_{i,j} (t_j - < x >)^2 \, p_{i,j} \tag{6}$$

$$\sigma^2_{x_1 t_1} = \sum_{i,j} (x_i - < x >)(t_j - < x >) \, p_{i,j} \tag{7}$$

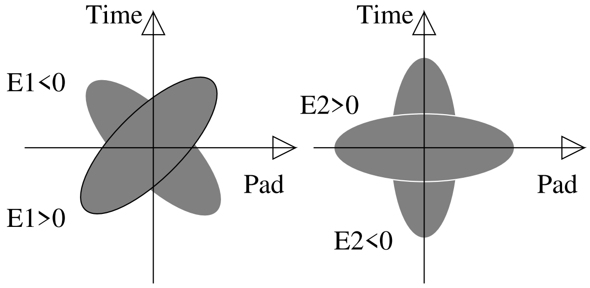

Figure 2: Orthogonal Quadrupole deformations in pad-time space

$$\epsilon_{L1} = \frac{tan(1.2\epsilon_1)}{tan(1.2)} \tag{8}$$

$$\epsilon_{L2} = \frac{tan(1.2\epsilon_2)}{tan(1.2)} \tag{9}$$

Rotate the x_1, t_1 coordinates by $\frac{\pi}{4}$ in order to find the second, orthogonal quadrupole moment. The second, rotated coordinate system is denoted by x_2, t_2.

$$\alpha_i = \frac{x_i - < x >}{\sqrt{2}} \tag{10}$$

$$\beta_j = \frac{t_j - < t >}{\sqrt{2}} \tag{11}$$

$$\sigma^2_{x_2} = \sum_{i,j} (\alpha_i + \beta_j)^2 \, p_{i,j} \tag{12}$$

$$\sigma^2_{t_2} = \sum_{i,j} (\alpha_i - \beta_j)^2 \, p_{i,j} \tag{13}$$

$$\sigma^2_{x_2 t_2} = \sum_{i,j} (\alpha_i + \beta_j) \, (\alpha_i - \beta_j) \, p_{i,j} \tag{14}$$

From these second moments one may define two orthogonal eccentricities which span an eccentricity space for cluster shape determination:

$$\epsilon_1 = \frac{\sigma^2_{x_1 t_1}}{\sigma_{x_1} \sigma_{t_1}} \tag{15}$$

$$\epsilon_2 = \frac{\sigma^2_{x_2 t_2}}{\sigma_{x_2} \sigma_{t_2}} \tag{16}$$

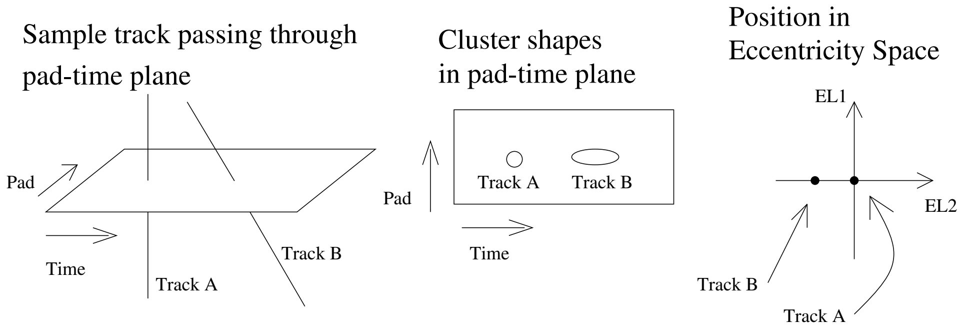

Figure 3: Physical interpretation of $(\epsilon_{L1}, \epsilon_{L2})$ space

Finally, because eccentricity is a highly nonlinear morphology measure, the two orthogonal eccentricities are linearized, and it is these linearized eccentricities which make up the substance of the following cluster analysis. Note that the parameter 1.2 was adapted from NA49, but could be changed in order to redistribute clusters in eccentricity space for STAR as needed.

3 Physical Meaning of the Morphology Measures

$(\epsilon_{L1}, \epsilon_{L2})$ both lie on a 2D space bounded by $+/-1$. $(0,0)$ is a perfectly symmetric object – a circle. Deviation from zero to positive or negative values in ϵ_{L2} measures oblateness or prolateness in the pad-time direction, respectively, and deviation in ϵ_{L1} measures the same quantity, but along a set of axes rotated $\frac{\pi}{4}$ from pad-time (Fig. 2).

Consider then two tracks passing through a pad-time plane, one at a dip angle of zero, i.e. perpendicular to the plane, labeled track A (fig. 3), and one at a large dip angle, which is labeled track B. Track A will then form a circular cluster shape in the plane, and track B an elliptical cluster shape. Thus the cluster morphology measures will find that track A is near $(0,0)$ in the space defined by $(\epsilon_{L1}, \epsilon_{L2})$, and Track B is displaced along the ϵ_{L2} axis, since it forms an ellipse with its major axis in the time direction.

Of course an actual cluster is non-circular in a much more extreme way than a simple ellipse, as will be seen in the following analysis. The further it is from $(0,0)$ in $(\epsilon_{L1}, \epsilon_{L2})$, the more eccentric it is.

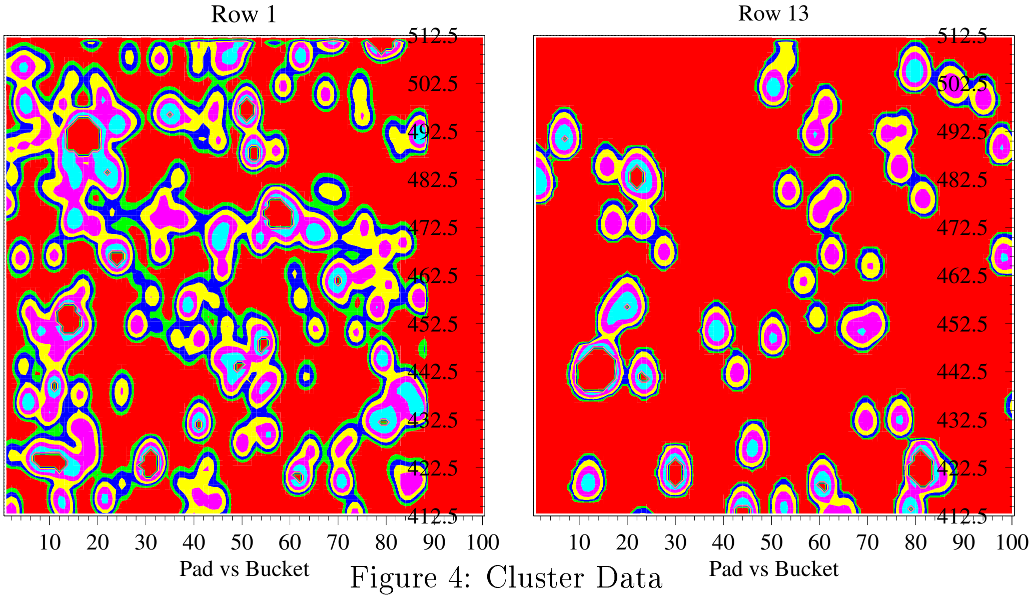

Figure 4: Cluster Data

4 Description of the Data

Venus and Hijing were both run through Geant to simulate Au+Au 200 GeV/nucleon collisions in the STAR detector system. Laser test data taken in September 1997 were used to compare with and calibrate Venus data. Magnetic field off data from Hijing were compared with magnetic field on data for Hijing.

Simulated cluster data for rows 1 and 13, i.e the innermost and outermost rows of the inner sector, are shown in figure 4. It should be noted how extremely dense the data are in row 1, so that one wonders if an entirely different set of algorithms than the ones currently used in STAR would be more desirable. The algorithms used in STAR are derived from TPC experiments in which the data were far less dense. One should also note the many plateaus which the mountain finder would not be able to resolve due to its dependence on the Raleigh Criterion. This too motivates one to explore other algorithmic possibilities.

The following per-cluster information is currently available from TCC: row number, sector number, total number of time sequences, total number of pixels, total number of pads, number of peaks found by the mountain finder, total charge, maximum charge, average charge, mean pad position, mean time position, σ_{x_1}, σ_{t_1}, $\sigma_{x_1 t_1}$, σ_{x_2}, σ_{t_2}, $\sigma_{x_2 t_2}$, ϵ_1, ϵ_2, ϵ_{L1}, ϵ_{L2}, all as defined in section 2, and mean x,y,z in TPC coordinates.

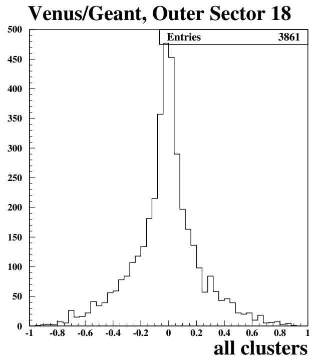

Figure 5: ϵ_{L1}

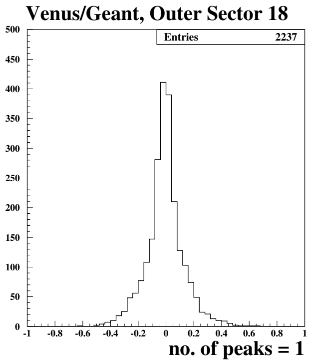

Figure 6: ϵ_{L1}

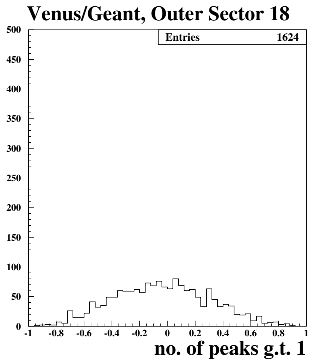

Figure 7: ϵ_{L1}

5 Analysis

To get a sense of the spread of clusters in eccentricity space, Venus data on a 1D histogram of ϵ_{L1} in outer sector 18 are plotted (Fig.5). Also shown are plots with cuts for number of peaks found by the mountain finder equal to one (Fig. 6) and number of peaks found by the mountain finder greater than one (Fig. 7). Scales and binnings have been kept the same for comparative purposes. As one would expect, the clusters found to have more than one peak are eccentric in shape and thus spread out across the range of ϵ_{L1}, while the other clusters, either because they passed the hit finder's triage cut, or because they did not pass the cut but were found by the mountain finder to have only peak, are sharply peaked near $\epsilon_{L1} = 0$. The tails in figure 6 are hypothesized to contain most of the merges that the mountain finder is unable to resolve due to its dependence on the Raleigh Criterion. By looking at plots of pad rms vs. time rms in pad-time space evidence was found that this is indeed the case.

Two-dimensional histograms contain the full eccentricity space information, as they are not projected out onto ϵ_{L1} or ϵ_{L2}. These plots were the principle ones used in the analysis. Accordingly, Venus data (Fig. 8) and laser test data (Fig. 9) are shown plotted in eccentricity space for outer sector 18. The laser test data are very sharply peaked in ϵ_{L1}. In ϵ_{L2} it has a similiar peak to the Venus data but slightly right shifted, with an additional tail trailing off towards $\epsilon_{L2} > 0$.

The sharp peak in ϵ_{L1} is simply because the laser test data are all straight tracks and is very sparse, so there are few merges and few very eccentric cluster shapes. The Venus data are correspondingly spread out in ϵ_{L1}. It has many merges. Even the unmerged tracks are curved and so make non-circular cluster

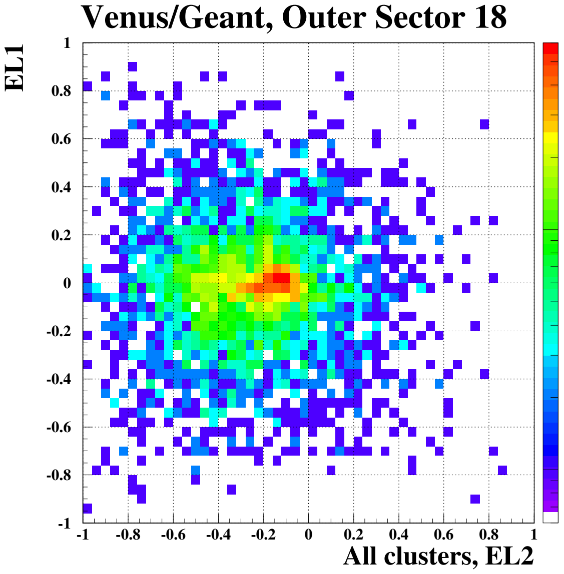

Figure 8: Eccentricity Space

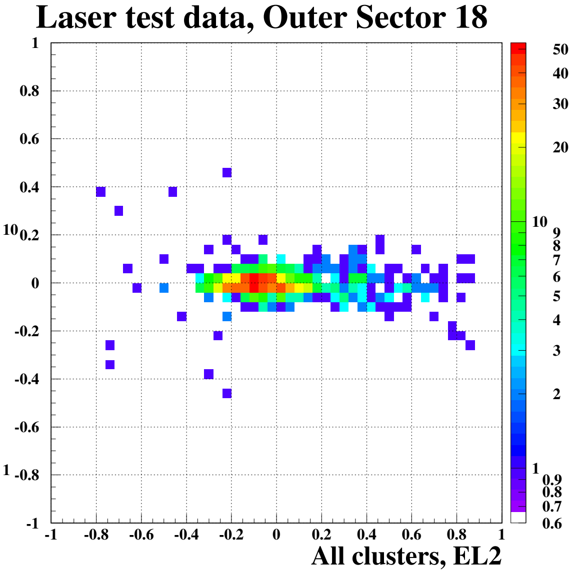

Figure 9: Eccentricity Space

shapes.

The merges are particularly noticeable when Hijng and Venus data from the inner sector are compared. Venus is known to have much more soft particle production. This leads to many more merges and a spreading out of the peak in eccentricity space in comparison to Hijing. This kind of diagnosis is useful for understanding the various relativistic heavy ion simulators on the cluster level in the TPC, and perhaps on other levels as well, as for example tracking and particle production.

The difference in the shape of the distribution in ϵ_{L2} is due to the lasers entering the TPC from the outside, i.e. from the last pad row, as opposed to tracks originating from the center of the TPC as with Venus. The laser tracks had nearly zero dip angles and had both positive and negative crossing angles, but in a tighter range than Venus, excepting two beams near the central x-y plane of the TPC. The Venus data had a full range of both dip angles and crossing angles.

Log plots were made of Venus data 1D projections onto ϵ_{L1} and ϵ_{L2} with cuts so as to select for the clusters with one peak, as determined by the hit finder code. On these then were sketched, by eye, a gaussian core with power law tails. It was assumed that the width of the peaks in eccentricity space were due either to merges or to charge drift in the tpc, that is, the fact that dip angle also broadens these peaks in ϵ_{L2} was for the moment disregarded. The gaussian core was hypothesized to derive mainly from charge drift error,

Percentage of Clusters				
Triage Cut	peaks=1	peaks>1	inside ellipse	outside ellipse
IS - passed	19	0	16	2
IS - didn't pass	44	37	39	43
OS - passed	40	0	34	6
OS - didn't pass	23	37	19	41

Table 1: Comparison of triage cut and proposed elliptical cut

whereas the power law tails represented the non-statistical error due to the Rayleigh Criterion resolution limit. This hypothesis worked well for everything except for ϵ_{L2} in the outer sector, where the somewhat amorphous shape made the hypothesis rather arbitrary.

From the intersection of the gaussian core and the power law tails in ϵ_{L1} and ϵ_{L2} the major and minor axes of an ellipse were defined. These in turn were used to make a cut which could be compared to the triage cut. The clusters lying inside the elliptical cut were near the center of the distribution in eccentricity space, so they would not be searched by the mountain finder if this elliptical cut were used instead of the triage cut. The clusters lying outside the ellipse were considered eccentrically shaped clusters, which should be searched for multiple peaks. The clusters which subsequently are found by the mountain finder to have only one peak would be tagged, so that they could be used in recursive tracking, two-hit merge deconvolution [5], or other downstream QA and analysis.

A quantitative analysis of the difference between the triage cut and the proposed elliptical cut was performed for the inner sector and the outer sector (table 1). The triage cut, literally a triangular cut (fig. 1), is a straight line drawn between $(3, 0)$ on the pad rms axis and $0, 3$ on the time rms axis. This can be set externally to a different value, but the staf parameter tables were checked after running a Venus/Geant simulation and it was found that, indeed, triage_rmscut was set to 3.

The percentage of clusters inside, or below the cut (passed), an outside, or above, the cut (didn't pass), are listed in the table for the inner sector (IS) and the outer sector (OS.) The columns, from left to right, show the percentage of the total clusters in the inner or outer sector, respectively, found by the hit finder code to have one peak and greater than one peak, and the percentage lying inside and outside the elliptical cuts.

The clusters that passed the triage cut and had one peak were never searched by the mountain finder. The clusters that didn't pass the triage cut and were found to have one peak are all either due to inefficiencies in the triage cut or inefficiencies in the mountain finder. This means that the peak finder is unnecessarily searching 44% of the clusters in the inner sector, a substantial inefficiency. The elliptical cut, as can be determined from the table with a simple calculation, would then represent a savings of 54% on the total number of clusters searched for multiple peaks in the inner sectors.

Thus 83% of the clusters in the inner sector are searched by the hit finder, whereas according to the proposed elliptical cuts only 45% would be searched, a savings of 45% in the number of peaks searched.

If the same calculation is made for the outer sector, it is found that the triage/mountain finder inefficiency is 23% of the total number of clusters. 60% of the clusters in the outer sector are searched by the mountain finder. The proposed elliptical cut for the outer sector would have the mountain finder search only 47% of the total number of clusters.

Thus the proposed elliptical cuts for the outer sector would represent a savings in the number of peaks searched by the mountain finder of 13% .

One could argue that the elliptical cut might have its own inefficiencies, in that some merges could be fairly circular. While this is true, by looking at pad rms vs. time rms plots equivalent to the one used by the triage cut (Fig. 1), it was found that this number is very small, certainly less than 10% , probably 1-2% . Further analysis could provide more precise quantitative numbers, though as this paper is intended to be a feasibility study this was not yet done at the time of writing.

Specific clusters were also tagged and looked at to see where they lay in the $(\sigma_{x2}, \sigma_{t2})$ space the triage cut used. A particular set of five or so clusters were found which highlighted the difference between the quadrupole morphology measure elliptical cuts and the simple triage cut. They were outside the proposed elliptical cut but were found to have one hit by the mountain finder. These clusters had a small rms in the time direction, but a large rms in the pad direction, so that they lay near to the σ_{x2}, or pad rms, axis. Thus they were, at the least, extremely curved tracks going in a special direction, and at the most irregularly shaped merges. The advantage of the elliptical cut, in a case such as this, is that, as mentioned above, if these clusters passed the peak-finding algorithm they could be tagged for special consideration later and searched by a different algorithm. And there is no disadvantage, because they get searched anyway, as opposed to using the triage cut and by the mountain finder ruling them out as being merges, despite their highly eccentric shape.

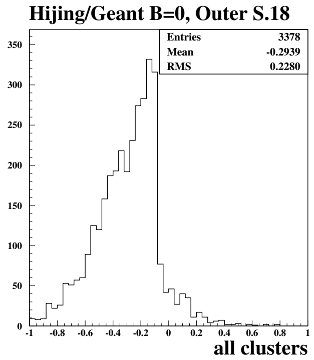

Figure 10: ϵ_{L2}

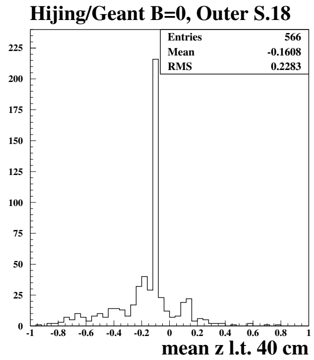

Figure 11: ϵ_{L2}

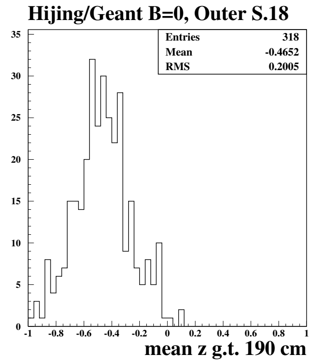

Figure 12: ϵ_{L2}

Some weeks after this quantitative analysis, the amorphous shape of ϵ_{L2} in the outer sector was explored. It was found that this unexpected shape was due to dip angle. That is, when cuts were made on the mean z position of the clusters in the TPC for Hijing/Geant with the magnetic field off (Fig. 10, 11, and 12), ϵ_{L2} became quite gaussian. ϵ_{L2} then corresponded to the authors' expectations from their experience with NA49, where it was found that single-hit clusters comprised an extremely sharp peak rising up out of a broad plain of merges in eccentricity space.

A 20 cm cut is used for the part of the tpc furthest from the collision center (Fig. 12), while a 40 cm cut is used for the part closest to the collision (fig. 11). One can clearly see the wider range of dip angles in the broadening of the peak in fig. 12, whereas even for a cut of twice the range the peak is extremely sharp in figure 11, as we would expect from the angular spread these cuts cover. The magnetic field is off so that all of the tracks are straight. We expect less merges in the outer sector both because of distance from the collision and because of straight tracks. Thus the identification of the former broadening of ϵ_{L2} with dip angle is not an unreasonable one.

6 Conclusion

The triage cut in use by the current hit finder code has not been optimized for algorithmic efficiency. As a cluster morphology measure it is somewhat simplistic, though admittedly it was not intended as such. The goal of investigating the quadrupole morphology measures was to gain a fuller picture of the clusters, not only as a basis for more efficient and more accurate hit finding, but also as a general diagnostic. In NA49, for example, there has been a great deal of internal debate about the track-vertex-finding code for the TPC. The quadrupole morphology measures have been useful in helping to unravel that puzzle.

Of course one does not expect the measures to be applied in exactly the same way for STAR. NA49 is a fixed-target experiment with a tight range of dip angles. A tight range of dip angles means a more limited range of cluster shapes. Because STAR is a central mid-rapidity collider experiment it has a wide range of dip angles, and thus many more possible cluster shapes. NA49 has a particle multiplicity of hundreds, perhaps 1200 charged particles spread out over six units of rapidity, while STAR has a multiplicity of three to five thousand spread out over two to three units of rapidity. Thus the merges in STAR are much more complicated, as has been shown above in section 5.

Even tentative, by eye elliptical cuts made without the consideration of dip angle effects show the improvements possible in peak-finding efficiency. Using the elliptical cuts rather than the triage cut would allow the peak finder to search about 45% less clusters in the inner sector and about 15% less clusters in the outer. One could argue that the elliptical cuts were simply tuned to get the percentages, but in fact they were made by independent criteria. The kumacs for the triage/elliptical cut comparison and the subsequent quantitative estimates were not written until after the elliptical cuts were fixed. In addition, a new set of elliptical cuts which are a function of mean z cluster position could improve the efficiency of the hit finder even more, particularly in the outer sector.

More than being just an improvement in processor time, the proposed cluster morphology measures give a wealth of information about cluster shapes, and are not themselves costly in compute time, particularly if they replace the triage cut calculation function in the hit-finder code. The information which these measures could provide include estimates of dip and crossing angle, improved track fitting and error measurements, improved identification of secondary tracks, and event by event variables like percolation and soft particle production. They also highlight the need for improved hit finding algorithms which are tailored to STAR data and give opportunity for clusters to be parsed out to different algorithms depending on their shape.

It is concluded that the quadrupole cluster morphology measures are worthy of further study and will work in STAR.

7 Future Direction

In NA49 several other of the variables available in TCC were used extensively in the hit finding code and definition of elliptical cuts, including total charge, maximum charge, and total number of pixels. These have yet to be utilized at STAR. It has been proposed at NA49 that two-hit merges may be found by cluster morphology measures and deconvoluted by inversion [5]. This may also be possible at STAR.

The resolution of eccentricity space when mean z cuts are applied should be mapped out and standardized, so that improved elliptical cuts and more precise quantitative estimates of the inefficiencies (i.e. number of circular-appearing merges) may be made. The applications of TCC to dip and crossing angle, track error, and secondary track finding need to be further expored.

Finally, benchmark tests need to be run on TCC and compared to the triage cut with respect to the use of the mountain finder and the run time of the cut-producing codes themselves.

References

[1] TCL and TPHAM, M.A. Lisa, R. Bossingham, et. al, STAR cluster/hit finder source code

[2] M.A. Lisa, Starnote 0238, “The STAR TPC Clusterfinder/Hitfinder,” (1996)

[3] T.A. Trainor, ”A Comparison of 1D x 1D and 2D Cluster Finders,” NA49 Note

[4] DIPT, D. Irmscher, NA49 cluster/hit finder source code

[5] T.A. Trainor, ”Cluster Deconvolution by Inversion,” NA49 Note